

Dual-emissions and thermochromic luminescences of isomorphic chiral twofold interpenetrated 3-D nets built from I^1O^2 type hybrid inorganic-organic frameworks of $[\text{NH}_2(\text{CH}_3)_2]_3[\text{Pb}_2\text{X}_3(\text{BDC})_2]$ ($\text{X} = \text{Br}, \text{I}$)

Shao-Xian Liu,^a Guo-Jun Yuan,^b Lu Zhai,*^a Lifeng Wang,^c Hong-Bin Luo,^a Xiao-Ming Ren*^{a,d,e}

^a State Key Laboratory of Materials-Oriented Chemical Engineering and College of Chemistry & Molecular Engineering, Nanjing Tech University, Nanjing 210009, P. R. China

^bSchool of Environmental Science, Nanjing Xiaozhuang University, Nanjing 211171, P. R. China

^c Institute for Frontier Materials (IFM), Deakin University, 75 Piggons Road, Waurn Ponds, Victoria 3216, Australia

^d College of Materials Science and Engineering, Nanjing Tech University, Nanjing 210009, P. R. China

^e State Key Lab & Coordination Chemistry Institute, Nanjing University, Nanjing 210023, P. R. China

Tel.: +86 25 58139476

Fax: +86 25 58139481

Email: zhailu@njtech.edu.cn (LZ); xmren@njtech.edu.cn (XMR)

Contents

Fig. S1 Photographs of crystals of (a) colorless **1a/1b** (b) light yellow **2a/2b**

Fig. S2 Experimental and simulated PXRD patters of (a) **1a/1b** and (b) **2a/2b**, respectively. The simulated PXRD patters are obtained from single crystal X-ray diffraction data using Mercury3.8 program for **1a** and **2a**

Fig. S3 IR spectra of **1a/1b** and **2a/2b**, respectively

Fig. S4 TG plots of **1a/1b** and **2a/2b**, showing quite similar thermal behaviors and four steps of losing weight processes in 300-1073 K. The hybrid crystals start to lose weight at ca. 448 K (175 °C) for **1a/1b** versus ca. 474 K (201 °C) for **2a/2b**

Fig. S5 (a) ORTEP view with the thermal ellipsoid at 50% probability level and (b) coordination pentagonal bipyramidal of PbBr₃O₄ in **1b**, where the symmetric codes: #1 = y, -1+x, 1-z; #2 = y, x, 1-z

Fig. S6 Helical polyhedral chain in (a) **1a** and (b) **1b**, which are comprised of pentagonal bipyramid dimmers and shows mirror-image relationship, respectively

Fig. S7 (a) ORTEP view with the thermal ellipsoid at 50% probability level and (b) coordination pentagonal bipyramidal of PbI₃O₄ in **2a**, where the symmetric codes: #1 = y, 1+x, 1-z; #2 = y, x, 1-z

Fig. S8 (a) ORTEP view with the thermal ellipsoid at 50% probability level and (b) coordination pentagonal bipyramidal of PbI₃O₄ in **2b**, where the symmetric codes: #1 = 2-y, 1-x, 0.5-z; #2 = 1-y, 1-x, 0.5-z

Fig. S9 Photographs of **1a/1b** single crystal under (a) visible light at 303 K and ultraviolet with λ = 340-380 nm at (b) 123 K (c) 143 K (d) 163 K (e) 183 K (f) 203 K (g) 223 K (h) 243 K (i) 263 K (j) 283 K (k) 303 K, which show color of emission alters with temperature change

Fig. S10 Photographs of **2a/2b** single crystal under (a) visible light at 303 K and ultraviolet with $\lambda = 340\text{-}380$ nm at (b) 163 K (c) 183 K (d) 203 K (e) 223 K (f) 243 K (g) 263 K (h) 883 K (i) 303 K, which show color of emission alters with temperature change

Table S1: Crystallographic data and refinement parameters for **1b** and **2b**

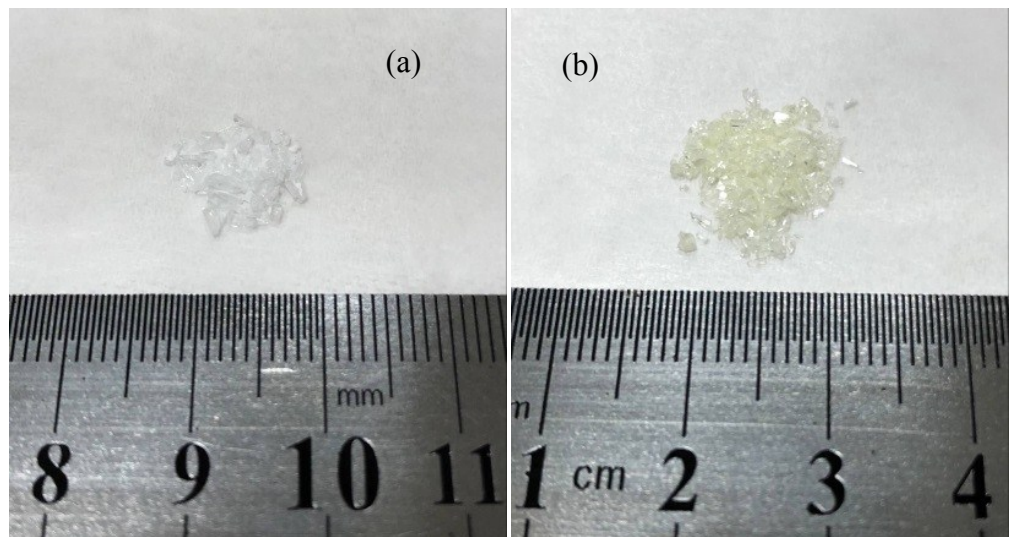


Fig. S1 Photographs of crystals of (a) colorless **1a/1b** (b) light yellow **2a/2b**.

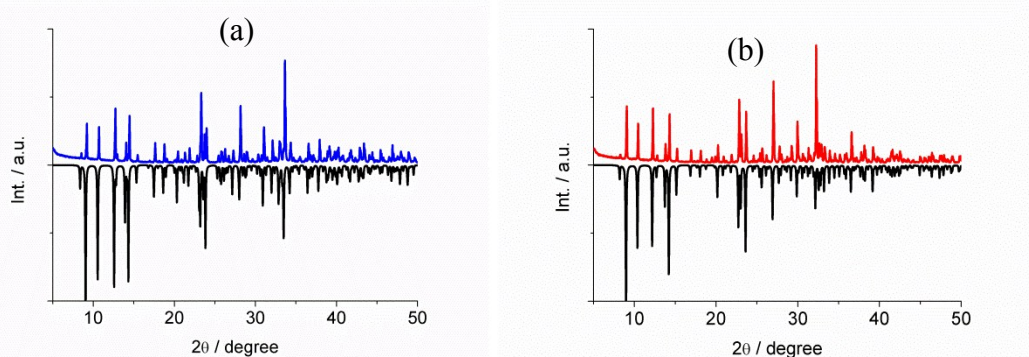


Fig. S2 Experimental and simulated PXRD patters of (a) **1a/1b** and (b) **2a/2b**, respectively. The simulated PXRD patters are obtained from single crystal X-ray diffraction data using Mercury 3.8 program for **1a** and **2a**.

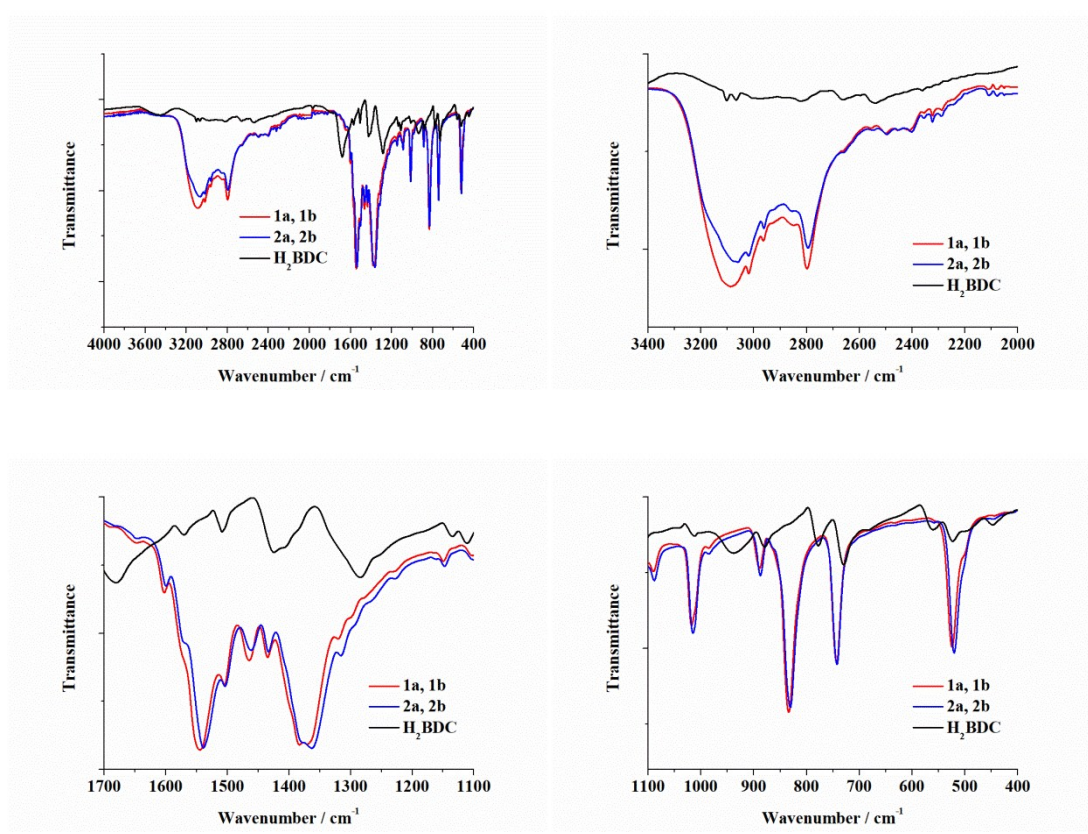


Fig. S3 IR spectra of **1a/1b** and **2a/2b**, together with the ligand, respectively.

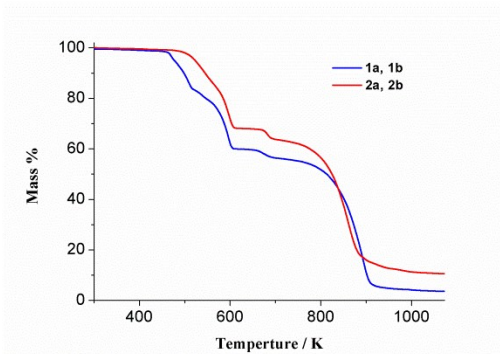


Fig. S4 TG plots of **1a/1b** and **2a/2b**, showing quite similar thermal behaviors and four steps of losing weight processes in 300-1073 K. The hybrid crystals start to lose weight at ca. 448 K (175 °C) for **1a/1b** versus ca. 474 K (201 °C) for **2a/2b**.

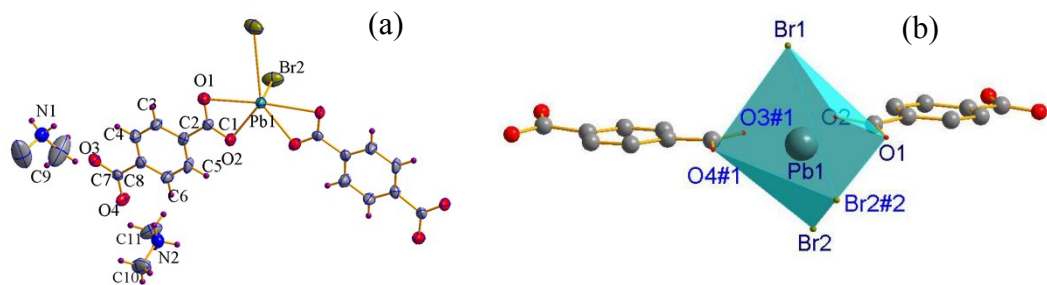


Fig. S5 (a) ORTEP view with the thermal ellipsoid at 50% probability level and (b) coordination pentagonal bipyramidal of PbBr_3O_4 in **1b**, where the symmetric codes: #1 = y, -1+x, 1-z; #2 = y, x, 1-z.

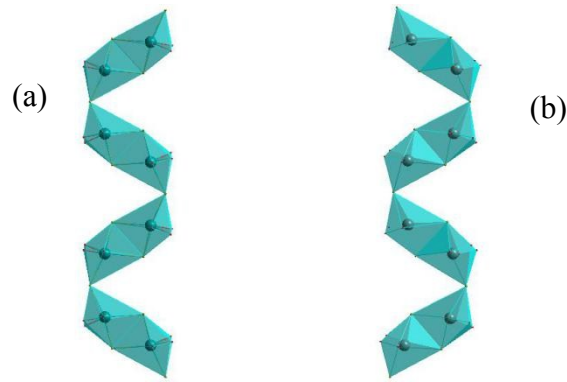


Fig. S6 Helical polyhedral chain in (a) **1a** and (b) **1b**, which are comprised of pentagonal bipyramid dimmers and shows mirror-image relationship, respectively.

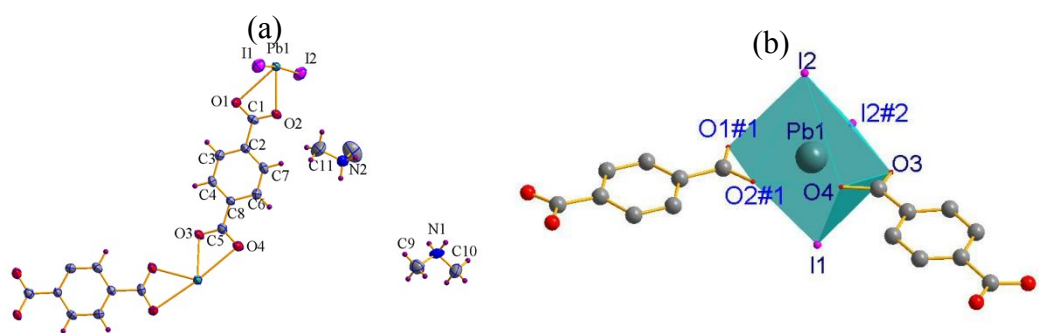


Fig. S7 (a) ORTEP view with the thermal ellipsoid at 50% probability level and (b) coordination pentagonal bipyramidal of PbI_3O_4 in **2a**, where the symmetric codes: #1 = y , $1+x$, $1-z$; #2 = y , x , $1-z$.

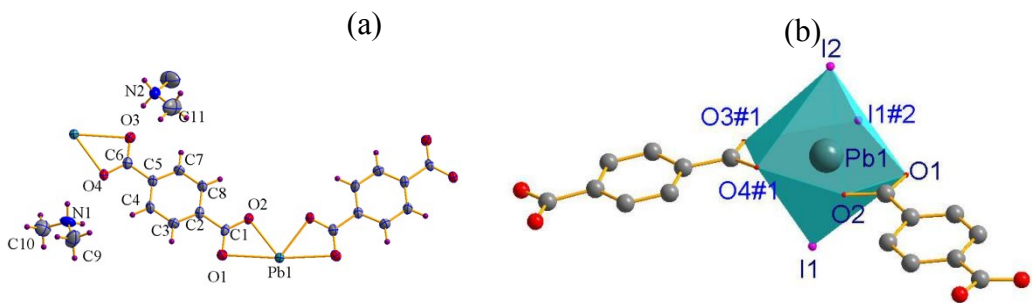


Fig. S8 (a) ORTEP view with the thermal ellipsoid at 50% probability level and (b) coordination pentagonal bipyramidal of PbI_3O_4 in **2b**, where the symmetric codes: #1 = 2- y , 1- x , 0.5- z ; #2 = 1- y , 1- x , 0.5- z .

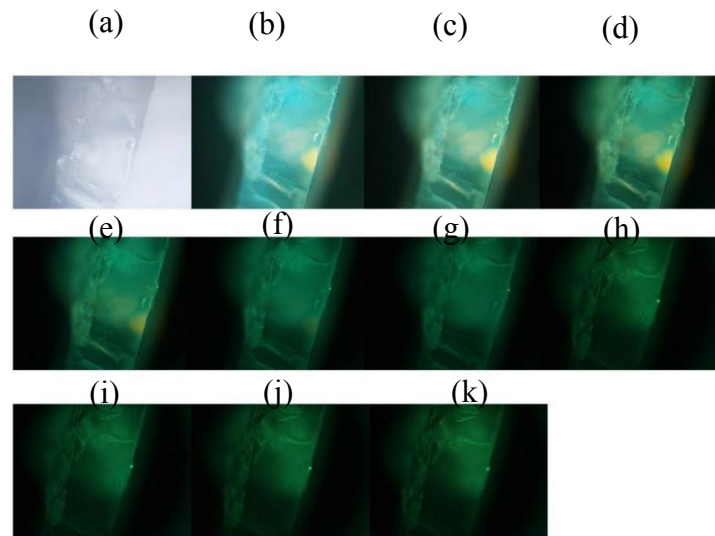


Fig. S9 Photographs of **1a/1b** single crystal under (a) visible light at 303 K and ultraviolet with $\lambda = 340\text{-}380$ nm at (b) 123 K (c) 143 K (d) 163 K (e) 183 K (f) 203 K (g) 223 K (h) 243 K (i) 263 K (j) 283 K (k) 303 K, which show color of emission alters with temperature change.

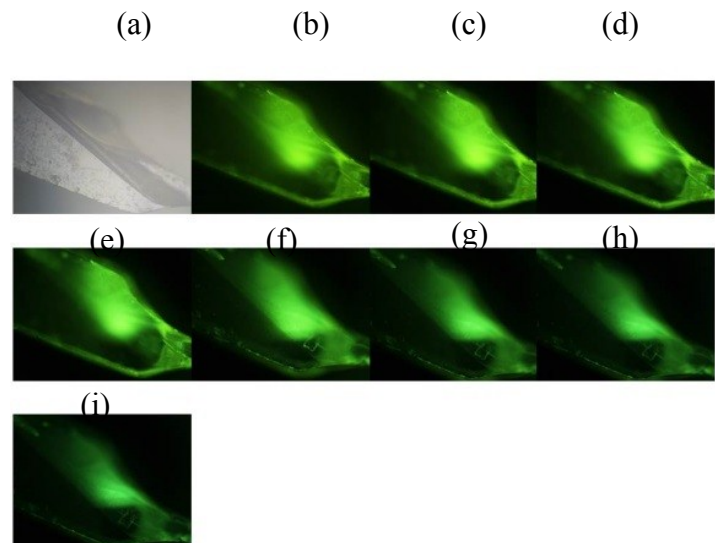


Fig. S10 Photographs of **2a/2b** single crystal under (a) visible light at 303 K and ultraviolet with $\lambda = 340\text{-}380$ nm at (b) 163 K (c) 183 K (d) 203 K (e) 223 K (f) 243 K (g) 263 K (h) 283 K (i) 303 K, which show color of emission alters with temperature change.

Table S1: Crystallographic data and refinement parameters for **1b** and **2b**

Compound	1b	2b
Temperature/K	295	278
Chemical formula	$C_{22}H_{32}Br_3N_3O_8Pb_2$	$C_{22}H_{32}I_3N_3O_8Pb_2$
Formula weight	1120.61	1261.59
Wavelength (Å)	0.71073	0.71073
Crystal system	Tetragonal	Tetragonal
Space group	$P4_12_12$	$P4_12_12$
<i>a</i> (Å)	13.8177(5)	13.9190(10)
<i>b</i> (Å)	13.8177(5)	13.9190(10)
<i>c</i> (Å)	16.3601(11)	17.003(3)
α (°)	90	90
β (°)	90	90
γ (°)	90	90
$V(\text{\AA}^3) / Z$	3123.6(3)/4	3294.1(7)/4
ρ (g·cm ⁻³)	2.383	2.544
F(000)	2071	2288
Abs. coeff. (mm ⁻¹)	14.649	13.063
Flack parameter	0.012(5)	0.022(5)
θ Ranges of data collection (°)	2.894-25.025 -16 ≤ <i>h</i> ≤ 16	2.927-27.558 -18 ≤ <i>h</i> ≤ 18
Index range	-16 ≤ <i>k</i> ≤ 16 -19 ≤ <i>l</i> ≤ 19	-18 ≤ <i>k</i> ≤ 18 -22 ≤ <i>l</i> ≤ 22
R_{int}	0.0495	0.0413
Independent reflections /restraints/parameters	2760/0/176	3771/0/177
Refine method	Full-matrix least-squares on F^2	
Goodness-of-fit on F^2	1.012	1.105

R_1 , wR_2 [$I > 2\sigma(I)$]	$R_1 = 0.0269$ $wR_2 = 0.0500$	$R_1 = 0.0171$ $wR_2 = 0.0364$
R_1 , wR_2 [all data]	$R_1 = 0.0336$ $wR_2 = 0.0517$	$R_1 = 0.0193$ $wR_2 = 0.0369$
Residual ($e \cdot \text{\AA}^{-3}$)	1.794/-0.525	0.503/-0.540

$$R_1 = \sum(|F_o| - |F_c|) / \sum|F_o|, wR_2 = \sum w(|F_o|^2 - |F_c|^2)^2 / \sum w (|F_o|^2)^2]^{1/2}$$